Steady-State Kinetic Studies of Superoxide Dismutases: Properties of the Iron Containing Protein from *Escherichia coli*[§]

Christopher Bull[†] and James A. Fee*[‡]

Contribution from the Biophysics Research Division and the Department of Biological Chemistry, The University of Michigan, Ann Arbor, Michigan 48109. *Received August 2, 1984*

Abstract: The catalysis of superoxide dismutation ($2O_2^- + 2H^+ \rightarrow O_2 + H_2O_2$) by iron superoxide dismutase from *Escherichia coli* has been examined with a specially constructed stopped-flow spectrophotometer. The disappearance of superoxide in the presence of the enzyme followed the velocity expression $-d[O_2^-]/dt = k_{fir}[O_2^-] + 2k_{sec}[O_2^-]^2 + 2[enz]TN[O_2^-]/(K_m + [O_2^-])$; numerical methods for extracting the Michaelis–Menten parameters, TN and K_m, from the data were developed. TN is independent of pH and, based on Fe concentration, is equal to $\sim 26\,000\ s^{-1}$ at 25 °C. K_m is independent of pH below 8 and increases tenfold per pH unit above 10. The apparent ionization controlling K_m has a $pK_a \sim 9.0$, and at pH 8.4 and 25 °C, K_m has a value of $\sim 80\ \mu M$. The activation parameters for TN and TN/K_m were determined. Previous results [Fee et al. *Isr. J. Chem.* **1981**, *21*, 54–58] suggested that water bound to Fe^{3+} hydrolyzed with $pK_a^o \sim 9$. Nevertheless, reduction of the iron caused the uptake of only one proton at any pH from 7 to 10, indicating the presence of an ionizable group close to the iron in reduced enzyme with pK_a^r near 9; the acid form of this group appears to promote binding of O_2^- to the reduced protein. Several anions were found to be competitive inhibitors. These fell into two classes: N_3^- and F^- which bind directly to the Fe^{3+} and ClO_4^-, SCN^-, Cl^-, $HCOO^-$, and SO_4^{2-} which appear not to bind to the Fe^{3+}. A mechanism of catalysis and of anion inhibition is presented which involves a reduction–oxidation cycle and accounts for all known equilibria involving the iron, including both classes of anionic inhibitors. Various general acids were shown to increase TN while not affecting TN/K_m. On this evidence, the rate-limiting step in catalysis is suggested to be proton donation from a general acid, most likely H_2O, to an enzyme–substrate intermediate.

There are three types of superoxide dismutases based on the metal ion involved in catalysis. The general properties, distribution, and possible biological functions of this disparate class of proteins and of superoxide have been discussed in various review papers.[1] The present article is concerned primarily with the mechanism of the iron superoxide dismutase from *Escherichia coli*. It is now generally accepted that metal ion catalyzed superoxide dismutation proceeds by a cyclic oxidation–reduction mechanism (reaction 1 and 2)

$$M^{n+} + O_2^- \rightarrow M^{(n-1)+} + O_2 \quad (1)$$

$$M^{(n-1)+} + O_2^- + 2H^+ \rightarrow M^{n+} + H_2O_2 \quad (2)$$

where M = Cu, Fe, or Mn and n corresponds to 2, 3, and 3, respectively, for each of the metals. This has been demonstrated for each type of superoxide dismutase[2] and for several smaller coordination compounds[3] which can also be effective catalysts. Questions remain, however, about the details of the catalytic processes. In the case of Cu/Zn protein, pulse radiolysis studies have suggested the reaction is diffusion limited and no rate-limiting first-order process has been observed.[2a] However, an indirect, polarographic measurement indicated that kinetic saturation of the Cu/Zn protein might occur.[4] Preliminary studies of the Fe protein from *E. coli* suggested that saturation occurred with some internal step becoming rate limiting[5] while the Mn protein shows a more complicated kinetic behavior which has been interpreted in terms of fast and slow cycles.[2d-f] In this report we utilize advances in instrumentation and data analysis which make it possible to examine the catalyzed dismutation reaction directly at initial superoxide concentrations up to ~ 4 mM and which allow accurate determinations of steady-state kinetic parameters.

A detailed picture of the active site of the iron superoxide dismutase is currently being developed. Recent X-ray crystallographic analyses at 3-Å resolution[6a,b] have shown the presence of four protein-to-iron ligand groups, one of which is histidine (His-26 in the *E. coli* protein). The identity of the others is not known due to lack of complete sequence data although imidazole and carboxylate functions are likely; physical measurements exclude tyrosine or sulfur ligands. NMR relaxation studies suggested the presence of a bound water molecule.[7a,b]

A number of physical measurements, including a partial bleaching of the 350-nm absorption band ($\epsilon = 1850\ M^{-1}\ cm^{-1}$)

[§] Supported by USPHS Grant GM 21519.

[†] Present address: Bio Products Department, Washington Research Center, W. R. Grace and Co., 7379 Route 32, Columbia, MD 21044.

[‡] Present address: Isotope and Nuclear Chemistry Division, INC-4, Mail Stop C345, Los Alamos National Laboratory, University of California, Los Alamos, New Mexico 87545. Address requests for reprints to this address.

(1) (a) Yamazaki, I.; Piette, L. H. *Biochim. Biophys. Acta* **1963**, *77*, 47–63. (b) Fridovich, I. *Acc. Chem. Res.* **1972**, *5*, 327–326. (c) Fridovich, I. In "Advances in Enzymology"; Meister, A., Ed.; Wiley: New York, 1974; Vol. 41, pp 35–97. (d) Bors, W.; Saran, M.; Lengfelder, E.; Spottl, R.; Michel, C. *Curr. Top. Radiat. Res. Q.* **1974**, *9*, 247–309. (e) Halliwell, B. *Cell. Biol. Int. Rep.* **1978**, *2*, 113–128. (f) Fee, J. A. In "Metal Ion Activation of Dioxygen"; Spiro, T. G., Ed.; Wiley: New York, 1980; pp 209–327. (g) Michelson, A. M., McCord, J. M., Fridovich, I., Eds. "Superoxide and Superoxide Dismutases"; Academic Press: London, 1977. (h) Fridovich, I. *Science (Washington, D.C.)* **1978**, *201*, 875–880. (i) Bannister, J. V., Hill, H. A. O., Eds. "Chemical and Biochemical Aspects of Superoxide and Superoxide Dismutase"; Elsevier/North Holland: Amsterdam, 1980. (j) Bannister, W. H., Bannister, J. V., Eds. "Biological and Clinical Aspects of Superoxide and Superoxide Dismutase"; Elsevier/North Holland: Amsterdam, 1980. (k) Fridovich, I. In "Oxygen and Oxy-Radicals in Chemistry and Biology"; Rodgers, M. A. J., Powers, E. L., Eds.; Academic Press: New York, 1981; pp 197–204, 221–239. (l) Fee, J. A. In "Oxygen and Oxy-Radicals in Chemistry and Biology"; Rodgers, M. A. J., Powers, E. L., Eds.; Academic Press: New York, 1981; pp 204–221, 221–239. (m) Fee, J. A. *Trends Biochem. Sci. (Pers. Ed.)* **1982**, *7*, 84–86. (n) Halliwell, B. *Ibid.* **1982**, *7*, 270–272.

(2) (a) Fielden, E. M.; Roberts, P. B.; Bray, R. C.; Lowe, D. J.; Mautner, G. N.; Rotilio, G.; Calabrese, L. *Biochem. J.* **1974**, *139*, 49–60. (b) Klug-Roth, D.; Fridovich, I., Rabani, J. *J. Am. Chem. Soc.* **1973**, *95*, 2786–2790. (c) Lavelle, F.; McAdam, M. E.; Fielden, E. M.; Roberts, P. B.; Puget, K.; Michelson, A. M. *Biochem. J.* **1977**, *161*, 3–11. (d) Pick, M.; Rabani, J.; Yost, F.; Fridovich, I. *J. Am. Chem. Soc.* **1974**, *96*, 7329–7333. (e) McAdam, M. E.; Fox, R. A.; Lavelle, F.; Fielden, E. M. *Biochem. J.* **1977**, *165*, 71–79. (f) McAdam, M. E.; Lavelle, F.; Fox, R. A.; Fielden, E. M. *Biochem. J.* **1977**, *165*, 81–87.

(3) Cf.: Bull, C.; McClune, G. J.; Fee, J. A. *J. Am. Chem. Soc.* **1983**, *105*, 5290–5300 and references therein.

(4) Rigo, A.; Viglino, P.; Rotilio, G. *Biochem. Biophys. Res. Commun.* **1975**, *63*, 1013–1018.

(5) Fee, J. A.; McClune, G. J.; O'Neill, P.; Fielden, E. M. *Biochem. Biophys. Res. Commun.* **1981**, *100*, 377–384.

(6) (a) Ringe, D.; Petsko, G. A.; Yamakura, F.; Suzuki, K.; Ohmori, D. *Proc. Natl. Acad. Sci. U.S.A.* **1983**, *80*, 3879–3883. (b) Stallings, W. C.; Powers, T. B.; Pattridge, K. A.; Fee, J. A.; Ludwig, M. L. *Proc. Natl. Acad. Sci. U.S.A.* **1983**, *80*, 3884–3888.

(7) (a) Villafranca, J. J.; Yost, F. J.; Fridovich, I. *J. Biol. Chem.* **1974**, *249*, 3532–3536. (b) Villafranca, J. J. *FEBS Lett.* **1976**, *62*, 230–232.

0002-7863/85/1507-3295$01.50/0

at high pH, suggest that the bound water of Fe^{3+}-dismutase may ionize (hydrolyze) with pK_a near 9 (reaction 3). The binding

$$P\text{-}Fe^{3+}\text{-}OH_2 \rightleftharpoons P\text{-}Fe^{3+}\text{-}OH^- + H^+ \quad (3)$$

of fluoride causes spectral changes similar to those observed at high pH,[8] in keeping with the similarity of OH^- and F^- as ferric ligands.[9] Azide also binds to the ferric ion, giving rise to two new bands in the visible spectrum at 440 nm (ϵ = 1660 M^{-1} cm^{-1}) and at 320 nm (ϵ = 3300 M^{-1} cm^{-1}).[8,10] Crystallographic analyses have shown that azide binds to a single coordination position of the Fe^{3+}.[6a,b] These results are consistent with a coordination site for water on the Fe^{3+} ion; the importance of such an open coordination position for metal ion catalysis of superoxide dismutation was discussed several years ago.[11]

Preliminary investigation of the steady-state properties of the enzyme have shown that the maximal turnover number is independent of pH while K_m is influenced by an ionization (pK_a = 8.8, basic form inactive).[5] Azide and F^- are also inhibitors,[8,11,12a-c] but cyanide is not.[7a,8] Azide inhibits competitively, and a distinct discrepancy between azide inhibition (K_I) and binding (K_d) was noted.[10,11] In this article we investigate this behavior and show that it arises as a natural consequence of the catalytic cycle of superoxide dismutases. Inhibition by several other anions is shown to be competitive with O_2^-, and the presence of an anion binding pocket near the iron[10] is confirmed. In addition we have found that the published redox potential[13] of iron superoxide dismutase is untrustworthy due to the apparent lack of reactivity of the mediators employed. The observed steady-state kinetics have been reconciled with all equilibria known for the protein, and a catalytic mechanism is proposed in which proton transfer from general acids within the solution to the protein is the rate-limiting step.

Materials and Methods

Superoxide dismutase concentrations (expressed on an active site basis) were determined from visible spectra with the following extinction coefficients ([metal]$^{-1}$ cm^{-1}): for Cu/ZnSD[14] 150;[15] for FeSD 1850;[8] and for MnSD 910.[16] Bovine Cu/ZnSD was purchased from Diagnostic Data, Inc. (Mountain View, CA), and used as received. FeSD was prepared from *E. coli* (Grain Products) as described by Slykehouse and Fee,[8] while MnSD was prepared from *Thermus thermophilus* as reported by Sato and Nakazawa.[15]

The stopped-flow apparatus and associated computer equipment have been described previously.[3,17] Briefly, the apparatus uses three driving syringes of 0.25-, 2.5-, and 2.5-mL capacity. Potassium superoxide, dissolved in a miscible organic solvent, generally with the aid of crown ether, is maintained in the small syringe, and appropriate buffer solutions are placed in the larger syringes. Typically, the O_2^- solution is mixed first with a weak buffer of pH ~10, and the resulting solution is combined with a strong buffer of the desired pH in the second mixer. When present, enzyme solutions were added in this last mixer. The dead time from the first mixer to the observation cell is 5 ms, while from the second mixer it is only 2 ms. The volume used per shot is 0.02, 0.2, and 0.2 mL from each syringe.

The concentration of the superoxide solution is generally adjusted to give $[O_2^-]_0 \sim$ 1–2 mM after mixing, but initial concentrations as high as 4 mM can easily be obtained. At this concentration of O_2^-, the resulting O_2 will not stay in solution at atmospheric pressure, but the dismutation reaction can be readily observed if the driving pressure is not released until the reaction is complete. For $[O_2^-]_0$ less than 2 mM, it is sufficient to degas the aqueous solutions on an aspirator. H_2O_2 is continuously removed from the superoxide stock solution by reaction with Me_2SO to give dimethyl sulfone,[18] so that immediately after mixing very little H_2O_2 is present. This reaction is slow in aqueous solutions, so at anytime after mixing the concentration of peroxide is half the concentration of superoxide that has decayed (cf. ref 3).

The concentration of superoxide was followed by using its absorbance in the UV. The following extinction coefficients (M^{-1} cm^{-1}) were determined at 10-nm intervals from 260 to 330 nm: 2080, 1490, 910, 534, 284, 133, 56, 33. Each kinetic trace, or "shot", consisted of either 151 or 401 data points. Four or more shots were averaged before storage to reduce noise. The observation path length was 2 cm, and the optical bandwidth was 3 nm.

Since Me_2SO freezes at 18 °C, a 2:1 mixture of Me_2SO and DMF was used below room temperature. Neat DMF is unsuitable due to limited solubility of O_2^-, even with crown ether, while acetonitrile forms a crystalline complex with crown ether.[19] These solvents were supplied by Burdick and Jackson and were sufficiently dry that they could be used as received.

Good's buffers[20] were obtained from Sigma and all aqueous solutions contained 10^{-4} M DETAPAC, which is better than EDTA in suppressing trace metal catalysis of superoxide dismutation.[3,21] 18-Crown-6 was obtained from PCR and KO_2 from Alfa.

Anion binding studies were done on a Perkin-Elmer Model 320 with 1-cm cuvettes thremostated at 25 °C or a Zeiss DMR-21 with 4-cm cuvettes held at 4 °C. Buffer solutions for these studies were identical with those of the stopped-flow activity studies, including organic solvent content (5% v/v). Buffer for F^- binding and inhibition contained 10% glycerol.[22] Binding data were analyzed with double-reciprocal plots.

Data Analysis. Superoxide decays spontaneously in aqueous solution by dismutation producing oxygen and hydrogen peroxide. Above pH 6, this reaction proceeds via formation of perhydroxyl radical (reactions 4 and 5. Therefore the dismutation rate is pH dependent and second order

$$HO_2 \rightleftharpoons H^+ + O_2^-;\ pK_a = 4.9 \quad (4)$$

$$HO_2 + O_2^- \rightarrow O_2 + HO_2^- \quad (5)$$

in superoxide (cf. ref 23a,b). Trace metals also catalyze the dismutation, and this process appears first order in superoxide, so therefore the decay of superoxide is given by expression 6

$$-\frac{d[O_2^-]}{dt} = k_{fir}[O_2^-] + 2k_{sec}[O_2^-]^2 \quad (6)$$

where k_{fir} is a general constant indicating the small amount of O_2^- decay by first-order processes and k_{sec} is the true rate constant for second-order dismutation of O_2^-. The concentration of superoxide can be determined as a function of time by monitoring the UV absorbance of superoxide. For such data, the derivative can be calculated at each data point, so that each point provides a separate equation relating the two unknown rate constants. Standard least-squares techniques are used to find the best values of k_{fir} and k_{sec}. The computational methods will be described elsewhere.[24]

Numerical differentiation generally causes a considerable increase in noise, so that other methods (e.g., nonlinear least-squares fitting of ab-

(8) Slykhouse, T. O.; Fee, J. A. *J. Biol. Chem.* **1976**, *251*, 5472–5477.
(9) Cotton, F. A.; Wilkinson, G. "Advanced Inorganic Chemistry"; Wiley Interscience: New York, 1980.
(10) Fee, J. A.; McClune, G. J.; Lees, A. C.; Zidovetski; R.; Pecht, I. *Isr. J. Chem.* **1981**, *21*, 54–58.
(11) Fee, J. A.; McClune, G. J. In "Mechanisms of Oxidizing Enzymes"; Singer, T. P., Ondarza, R. N., Eds.; Elsevier/North Holland: Amsterdam, 1978; pp 273–283.
(12) (a) Misra, H. P.; Fridovich, I. *Arch. Biochem. Biophys.* **1978**, *189*, 317–322. (b) Asada, K.; Yoshidawa, K.; Takahashi, M.-A.; Maeda, Y.; Enmanji, K. *J. Biol. Chem.* **1975**, *250*, 2801–2807. (c) Yamakura, F. *Biochim. Biophys. Acta* **1976**, *422*, 280–294.
(13) Barrette, W. C., Jr.; Sawyer, D. T.; Fee, J. A.; Asada, K. *Biochemistry* **1983**, *22*, 624–627.
(14) Abbrevations used: SD, superoxide dismutase; EDTA, ethylenediaminetetraacetic acid; DETAPAC, diethylenetriaminepentaacetic acid; DCPIP, dichlorophenolindophenol; DMF, dimethylformamide; TN, turnover number.
(15) McCord, J. M.; Fridovich, I. *J. Biol. Chem.* **1969**, *244*, 6049–6055.
(16) Sato, S.; Nakazawa, K. *J. Biochem.* **1978**, *83*, 1165–1171.
(17) McClune, G. J.; Fee, J. A. *Biophys. J.* **1978**, *24*, 65–69.
(18) Gampp, H.; Lippard, S. J. *Inorg. Chem.* **1983**, *22*, 357–358.
(19) Gokel, G. W.; Cram, D. J.; Liotta, C. L.; Harris, H. P.; Cook, F. L. *J. Org. Chem.* **1974**, *39*, 2445–2446.
(20) (a) Good, N. E.; Winget, G. D.; Winter, W.; Connolly, T. N.; Izawa, S.; Singh, R. M. M. *Biochemistry* **1966**, *5*, 467–477. (b) Good, N. E.; Izawa, S. *Methods Enzymol.* **1968** *24*, 53–68.
(21) McClune, G. J. Ph.D. Dissertation, The University of Michigan, 1979. Available from University Microfilms, Ann Arbor, MI. McClune found that polyaminocarboxylato complexes of Fe catalyze superoxide dismutation with relative efficiency: CyDTA > HEDTA > EDTA > DETAPAC.
(22) Previously reported results[8] suggested that two azide or two fluoride ions could simultaneously bind to the Fe^{3+} of FeSD. It was later found that including a small amount of organic solvent in the medium completely prevented the spectral manifestations assigned to the binding of the second anion and that the expression of these effects was more apparent in some preparations of the protein than in others. (Unpublished observations of J. A. Fee.) Further, crystallographic studies[6a,b] showed evidence for only one azide bound to the metal. Thus, since all solutions used in this work contained 5% Me_2SO, it will be assumed that only one coordination position of the metal is involved in catalysis of superoxide dismutation. Also, a previous indication from this laboratory[8] that azide was not an inhibitor of FeSD is clearly incorrect.[11,12a]
(23) (a) Bielski, B. H. J. *Photochem. Photobiol.* **1978**, *28*, 645–649. (b) Bielski, B. H. J.; Allen, A. O. *J. Phys. Chem.* **1977**, *81*, 1048–1050.
(24) Bull, C.; Fee, J. A., manuscript in preparation.

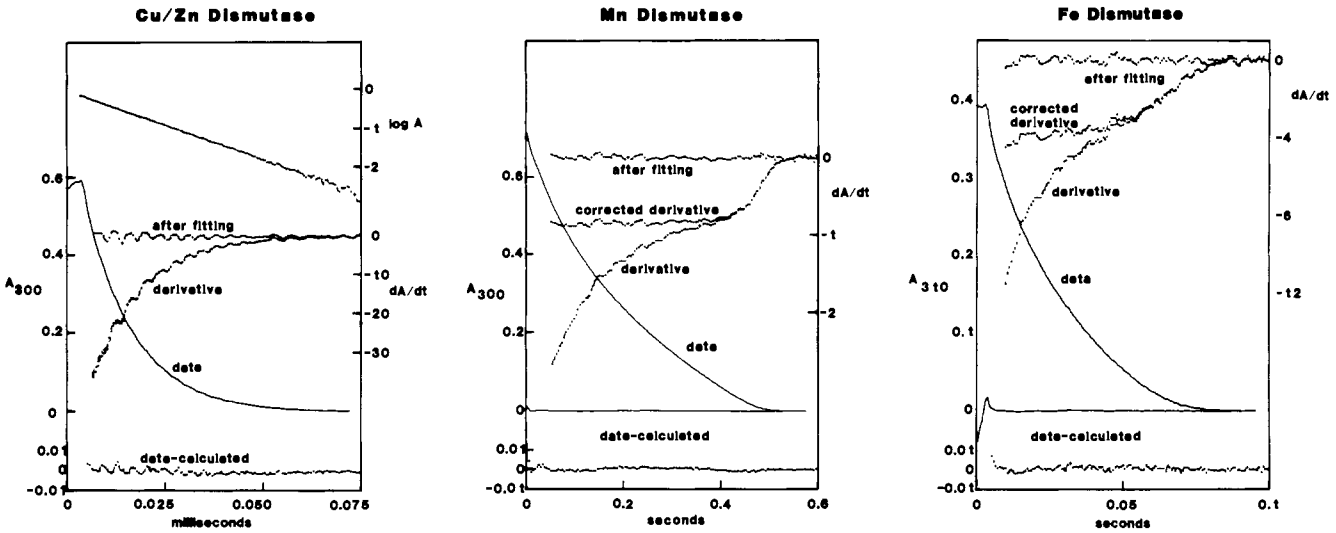

Figure 1. Superoxide decay catalyzed by three enzymes: Cu/ZnSD (left panel), Mn/SD (center panel), and FeSD (right panel). In each panel the following are shown: the absorbance vs. time data; the derivative of the data; the derivative data corrected for non-enzymatic dismutation to leave the enzyme-catalyzed component; the corrected derivative data minus the computer-fitted enzymatic component, i.e., the velocity residuals; and finally the difference between the data and the numerically simulated reaction, i.e., the absorbance residuals. In the left panel (Cu/ZnSD), the corrected derivative is virtually superimposed on the derivative data. The inset in this panel shows the linearity of a semilogarithmic plot of the original data. Enzyme concentrations were as follows: Cu/Zn, 0.3 μM; MnSD, 0.6 μM; and FeSD, 1.1 μM. Cu/ZnSD and MnSD were done at 25 °C in 0.2 M glycine buffer, pH 9.7, while the FeSD data were taken at 3 °C in 0.05 M TAPS, pH 8.4 (warm), also 0.05 M in KCl.

sorbance data) might be thought preferable. However, by maximizing signal to noise in the absorbance data, first by instrumental design and second by averaging several independent shots, the signal-to-noise ratio in the velocity data can be quite acceptable. The method is simple to program and rapid in execution, but its main advantage is the ease it offers in analyzing a velocity expression such as eq 7.

In the presence of superoxide dismutases, the rate of superoxide decay is given by eq 7. Again the derivative of the data may be calculated at

$$-\frac{d[O_2^-]}{dt} = k_{fir}[O_2^-] + 2k_{sec}[O_2^-]^2 + \frac{2[enz]TN[O_2^-]}{K_m + [O_2^-]} \qquad (7)$$

each point. Since k_{fir} and k_{sec} are known from experiments done in the absence of enzyme, their contribution to the derivative at each point is easily calculated and removed from the derivative, leaving a corrected derivative which is due only to the added enzyme. Nonlinear least-squares methods may be used to find values of TN and K_m which best fit this corrected derivative. When the value of K_m is greater than ~2 mM then one is restricted to analyzing for TN/K_m.

The quality of fit may be judged by substituting k_{fir}, k_{sec}, TN, and K_m back into eq 7, calculating the predicted velocity at each point, and removing this from the observed velocity. These velocity residuals should be randomly distributed around zero. In addition, the entire reaction may be simulated numerically and subtracted from the original data. These absorbance residuals should also exhibit no trends.

Results

Saturation Behavior of Superoxide Dismutases. Our data for Cu/ZnSD show no evidence of saturation (Figure 1, left panel), consistent with previously published pulse radiolysis studies.[2a] These data were taken with a relatively high concentration of enzyme, so that the corrections to the derivative are small. The enzymatic contribution is accurately fit by a simple first-order process. Because the contribution of spontaneous dismutation to the reaction is so small, a semilog plot of the absorbance data is linear (see inset, left panel). The derived second-order rate constant for the reaction of superoxide with the enzyme is 2×10^9 M^{-1} s^{-1} (based on Cu), in excellent agreement with pulse radiolysis results taken at much lower O_2^-.[25]

On attempting to fit these data to an enzymatic form, the program did not converge on unique values for TN and K_m. Instead the absolute values of TN and K_m increase without bound, while the ratio of TN/K_m remains constant and equal to the rate constant found by assuming a first-order process. Our experience with the iron enzyme and with simulated data has shown that, for a saturable enzyme, even with K_m several times greater than the initial O_2^- concentration, fitting to an enzymatic form leads to convergence, while fitting to a first-order process leaves characteristic trends in both velocity and absorbance residuals. Thus, if the Cu/ZnSD saturates, K_m must be greater than 5 mM O_2^-.

These data were taken under conditions quite similar to those used previously in the indirect polarographic method which reported a K_m near 0.5 mM.[4] Since our direct measurement covers superoxide concentrations much higher than this without any sign of saturation, the indirect result must be artifactual. The minimum value of K_m of 5 mM implies that the rate of any superoxide-independent steps in the catalytic cycle of Cu/ZnSD must exceed 5×10^6 s^{-1}. This is a lower limit for the rate at which electron and proton transfers occur near the Cu of the Cu/Zn protein.

Data for MnSD from *T. thermophilus* are also shown in Figure 1 (center panel). Saturation of the enzyme is clearly evident in the corrected derivative where the catalyzed velocity is constant over a wide range of superoxide concentration. These data were taken with a relatively low concentration of enzyme to illustrate how well the non-enzymatic contribution can be removed from the derivative. Derived constants for these data were TN = 1300 s^{-1} and K_m = 3 μM. We are presently pursuing a detailed study of the manganese protein, and no further data are reported here.

Data for FeSD at 3 °C are shown in the right panel of Figure 1. Again saturation behavior is evident in the corrected derivative, although it occurs at much higher O_2^- concentrations than with MnSD. Fitting to the enzymatic form gives satisfactory plots of residuals with TN = 7500 s^{-1} and K_m = 100 μM. These derived constants depend on temperature, pH, buffer, and anion concentrations. Before examining these effects in detail, several aspects of the method and some control experiments are described.

Validity of the Methods. This procedure of data analysis is related to integrated rate methods in that the entire reaction is used to obtain the rate constants.[26] Therefore the derived rate constants could be influenced by product inhibition or enzyme instability. Since the iron enzyme in particular is known to be inactivated by H_2O_2,[27] considerable effort was made to rule out possible artifacts. For FeSD, the TN and K_m did not depend on the initial O_2^- concentration in the range 0.2 to 2 mM (the initial

(25) McAdam, M. E. *Biochem. J.* **1977**, *161*, 697–699.

(26) Cornish-Bowden, A. "Principles of Enzyme Kinetics"; Butterworths: London, 1976.

(27) Asada, K.; Yoshikawa, K.; Takahashi, M.; Maeda, Y.; Enmanji, K. *J. Biol. Chem.* **1975**, *250*, 2801–2807.

concentration should not be much less than K_m if a reliable determination of TN and K_m is desired). Both TN and K_m were independent of enzyme concentraton. Adding H_2O_2 (8 mM) in the first aqueous syringe (enzyme in second aqueous syringe) changed neither TN or K_m for high concentrations of enzyme. Inactivation by H_2O_2 appears to occur relatively slowly over several minutes (depending on H_2O_2 concentration), while the entire O_2^- reaction occurs in less than a second. Inactivation of the iron protein became apparent as distinct trends in both velocity and absorbance residuals only at high pH with low concentrations of enzyme where the reaction time approached a minute; such conditions were avoided in this study. The activities of MnSD and Cu/ZnSD were also independent of H_2O_2 accumulation. Initial oxygen concentrations of 0 and 2 mM gave identical results for all three enzymes. Thus, for the short reaction times and final H_2O_2 concentrations, less than 1 mM used in this study, product inhibition and enzyme instability presented no problem for data analysis. These observations rule out the formation of a stable peroxo complex similar to the Fe-EDTA system.[3]

Values of TN and K_m proved to be sensitive to choice of buffer and anion concentration. The Good's buffers[20] used in this study had much less effect than carbonate or pyrophosphate. The apparent K_m increased slightly with increasing buffer concentration, e.g., at pH 8.4 in 0.2 M TAPS, K_m(app) was 150 μM, where extrapolating the values obtained at lower concentrations to zero buffer gave a K_m of 75 μM. Generally buffer concentrations of 0.05 or 0.1 M were used; this small effect was not investigated further.

Data sets collected at several different temperatures are presented. This is partly due to technical problems with the apparatus. However, since K_m decreases with temperature and is thus more accurately resolved in the numerical analysis, those perturbations which increase K_m were usually done at the lowest possible temperature.

Steady-State Analysis of Iron Superoxide Dismutase. In the dismutases, as in catalase, two molecules of substrate add to the enzyme in each cycle. This will lead to steady-state expressions with terms containing the square of substrate concentration *unless* the two substrate addition steps are irreversibly connected. Since simple Michaelis–Menten kinetics fit the data very well and since no evidence of product inhibition could be found, we assume that the reaction cycle consists of irreversible reductive and oxidative half-reactions. Scheme I shows the simplest scheme which can be written (neglecting protons for the moment). Both half-reactions have been written with Michaelis complexes (in brackets) because one such saturable step must exist, although its location is not known.

Scheme I

$$E_{ox} \underset{k_{-1}}{\overset{k_1O_2^-}{\rightleftharpoons}} [E_{ox}O_2^-] \xrightarrow{k_2} E_{red} + O_2$$
$$E_{red} \underset{k_{-3}}{\overset{k_3O_2^-}{\rightleftharpoons}} [E_{red}\cdot O_2^-] \xrightarrow{k_4} E_{ox} + H_2O_2 \qquad (8)$$

The expression for the steady-state kinetics of Scheme I may be derived by the method of King and Altman.[28] Following

$$-\frac{d[O_2^-]}{dt} = \frac{2[enz](1/k_2 + 1/k_4)^{-1}[O_2^-]}{\left[\dfrac{1}{k_{-1}}\dfrac{k_2}{k_{-1}+k_2} + \dfrac{1}{k_3}\dfrac{k_4}{k_{-3}+k_4}\right]^{-1}} + [O_2^-] \qquad (9)$$

Cleland,[29] the terms $k_2/(k_{-1} + k_2)$ and $k_4/(k_{-3} + k_4)$ represent the commitment to catalysis of the Michaelis complexes in the reductive and oxidative half-reactions, respectively. One may

(28) See: Segel, I. H. "Enzyme Kinetics"; Wiley-Interscience: New York, 1975; Chapter 9.
(29) Cleland, W. W. *Biochemistry* 1975 14, 3220–3224.

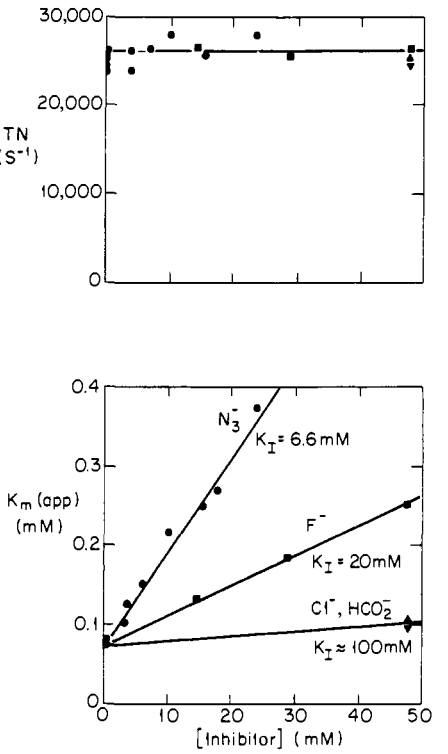

Figure 2. Effect of various anions on the TN and K_m of FeSD. Circles indicate azide, squares fluoride, triangles chloride, and inverted triangles formate. Conditions: 0.1 M TAPS, pH 8.4, 25 °C, initial $[O_2^-]$ = 1 mM.

define k_r and k_o as the productive binding rates of the reductive and oxidative half-reactions

$$k_r = k_1\left(\frac{k_2}{k_{-1} + k_2}\right) \qquad (10)$$

$$k_o = k_3\left(\frac{k_4}{k_{-3} + k_4}\right) \qquad (11)$$

and rewrite (9) to obtain

$$-\frac{d[O_2^-]}{dt} = \frac{2[enz](1/k_2 + 1/k_4)^{-1}[O_2^-]}{\dfrac{(1/k_2 + 1/k_4)^{-1}}{(1/k_r + 1/k_o)^{-1}} + [O_2^-]} \qquad (12)$$

hence

$$TN = (1/k_2 + 1/k_4)^{-1} \qquad (13)$$

and

$$K_m^{app} = \frac{(1/k_2 + 1/k_4)^{-1}}{(1/k_r + 1/k_o)^{-1}} \qquad (14)$$

Inhibition by Anions. Certain anions are inhibitors of iron superoxide dismutase. Illustrative data are shown in Figure 2. As expected for competitive inhibition, TN is independent of inhibitor concentration while the apparent K_m increases linearly with inhibitor concentration. For the several anions studied the effectiveness of inhibition decreases in the order $N_3^- > F^- > SCN^- > ClO_4^- > Cl^- > SO_4^{2-}$. Of these anions, only N_3^- and F^- demonstrably bind to the ferric form of the enzyme causing a perturbation of its spectral properties[8] and providing a possible mechanism for inhibition. In contrast, the other anions (SCN^-, ClO_4^-, Cl^-, and SO_4^{2-}) cause no (or minor) changes in the optical or EPR properties of the Fe^{3+} at inhibitory concentrations (data not shown), suggesting they do not bind directly to Fe^{3+}. The binding of these anions to the surface of the protein such that access to the Fe^{3+} is blocked has previously been suggested as the

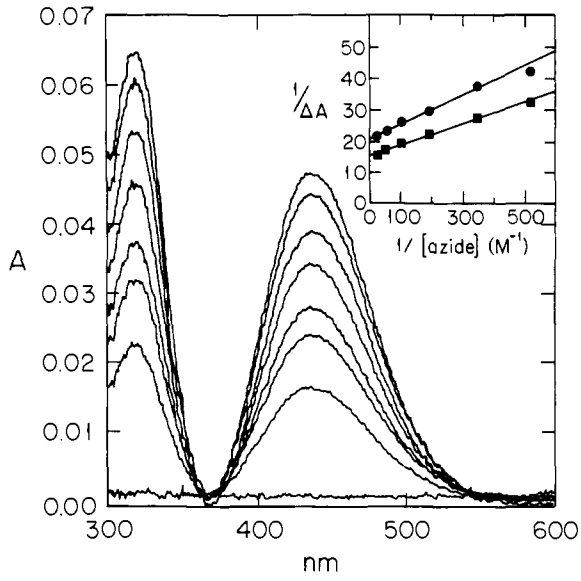

Figure 3. Difference spectra induced by adding azide to oxidized enzyme. Conditions: 0.1 M TAPS, pH 8.4, 25 °C, [FeSD] = 59 μM, initial volume 0.41 mL, 1 cm path length. Subsequent to the base line are three consequetive additions of 2 μL each of 0.2 M azide followed by single additions of 1, 2, and 4 μL of 1 M azide. The inset shows a reciprocal plot of 320 (circles) and 440 nm (squares) absorbance data.

basis of their inhibitory properties.[10] Thus, there are at least two classes of anion inhibitors, and the factors leading to competitive inhibition are evidently complicated. We will make the simplifying assumption that N_3^-, F^-, and OH^- do not bind to the Fe^{2+} of the protein. This assumption is generally supported by the much greater tendency of Fe^{3+} over Fe^{2+} to form complexes.[9] The two classes of inhibitors will be discussed separately.

Comparison of K_I and K_d for Azide. Preliminary results indicated that K_I was significantly greater than K_d for azide.[10,11] For the present conditions (see Figure 2) K_I = 6.6 mM. Difference spectra generated on binding azide to the oxidized form of the protein under identical experimental conditions are shown in Figure 3, and the reciprocal plots (inset) yield K_d = 2.3 mM. The following considerations offer a simple explanation for this apparent discrepancy.

Assuming N_3^- binds rapidly and reversibly only to the Fe^{3+} to cause competitive inhibition, the steady-state behavior is described by

$$\frac{d[O_2^-]}{dt} = \frac{2[enz](1/k_2 + 1/k_4)^{-1}[O_2^-]}{(1/k_2 + 1/k_4)^{-1}\left[\frac{1 + ([I]/K_d)}{k_r} + \frac{1}{k_o}\right]^{-1} + [O_2^-]} \quad (15)$$

from which the apparent K_m term can be rearranged to

$$K_m^{app} = \frac{(1/k_2 + 1/k_4)^{-1}}{(1/k_r + 1/k_o)^{-1}}\left(1 + \frac{[I]}{K_d}\cdot\frac{k_o}{k_o + k_r}\right) \quad (16)$$

yielding

$$K_I = K_d\cdot\frac{k_o + k_r}{k_o} \quad (17)$$

Thus, for the case in which the inhibitor binds to only one form of the enzyme, K_I should in general not equal K_d, and this result should be applicable to all superoxide dismutases or any enzyme where substrate enters the reaction cycle twice while the inhibitor binds to only one form. Returning to the experimental result that $K_I \simeq 3.0K_d$, eq 17 suggests that k_r must be roughly twice as great as k_o. These reactions are much too rapid to be observed with our stopped-flow apparatus, but this prediction may be testable with pulse radiolysis techniques.

Table I. Thermodynamic Parameters

reaction	E_a, cal/mol	PZ	ΔH^*, cal/mol	ΔS^*, cal/(deg·mol)
k_{sec} for O_2^-	4600	7.0×10^7	4000[a]	−25[b]
TN of FeSD	7920	1.5×10^{10}	7300[c]	−14
TN/K_m of FeSD	3960	1.9×10^{11}	3400[d]	−8.9

[a] The heat of ionization of TAPS is 4000 cal/mol; these data were corrected for the resulting pH shift of the buffer. [b] At pH 8.4. Since the reaction is pH dependent, due to the prior protonation, ΔS^* decreases 4.6 cal/(deg·mol) for each pH unit increase. [c] TN is independent of pH. [d] TN/K_m was measured 0.5 pH unit below the apparent pK_a affecting K_m. This apparent pK_a had a similar heat of ionization to TAPs buffer, so no correction is necessary.

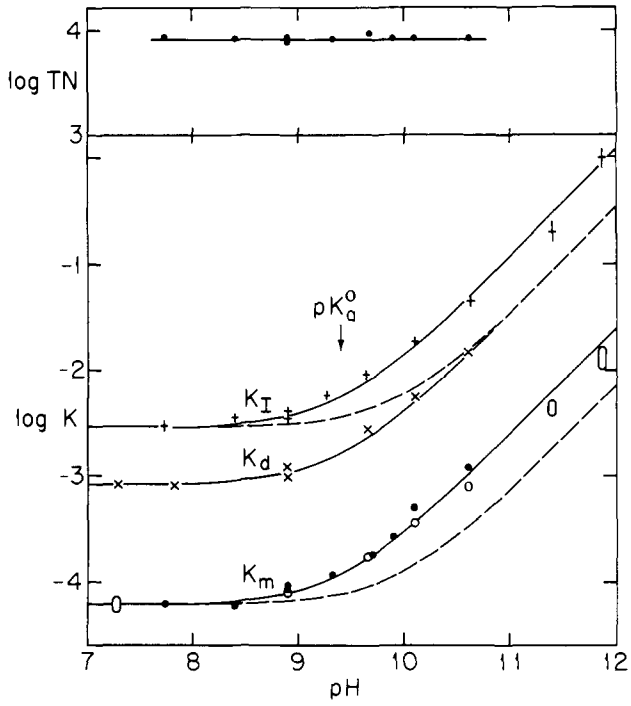

Figure 4. Variation with pH of steady-state kinetic parameters and the azide dissociation constant and inhibition constant. Filled circles show TN (upper panel) and K_m (lower panel) in the absence of azide, × symbols show the azide dissociation constant for oxidized enzyme, and + symbols show the azide inhibition constant. The arrow indicates the static pK_a^0 observed in the oxidized enzyme under the assay conditions 0.05 M buffer, 0.3 mM initial superoxide, 1 μM FeSD, 4 °C. Data for filled circles were taken under conditions where $[O_2^-]_0 > K_m$ thus allowing independent determination of K_m and TN. Data for open symbols were taken with $[O_2^-] \ll K_m$ resulting in an exponential decay characterized by TN/K_m. K_m was then calculated with the assumption that TN is constant. K_I was also determined by this method except a complete analysis was done at pH 8.9. The lower dashed line was calculated from eq 20 by assuming $K_a^r = 0$ and [I] = 0 while the upper dashed line was calculated with eq 17 under the assumption that $K_a^r = 0$. These show the expected results of having an ionizing group only in the oxidized form of the enzyme.

Examination of the pH dependence of the steady-state kinetic parameters as well as K_I and K_d for azide led us to an interesting new insight into the mechanism of FeSD. Partly for technical reasons, these experiments were done at lower temperatures. The following section threfore describes the temperature as well as the pH dependence of the FeSD-catalyzed dismutation reaction.

Effects of Temperature and pH on TN, K_m, and Azide Binding and Inhibition. TN and TN/K_m were determined in the temperature range 4 to 48 °C in TAPS buffer having a measured pH of 8.4 at 25 °C. Arrhenius plots were linear, suggesting no apparent change in mechanism over this temperature range, and the derived thermodynamic quantities are presented in Table I (cf. ref 30).

Values of TN and K_m as well as K_d and K_I for azide were determined as a function of pH at 4 °C; these are plotted in Figure

4. The data show the general features of those determined at 25 °C.[5] Thus, TN is independent of pH, $K_I \simeq 3.0K_d$ for azide, and the apparent pK_a affecting K_d, K_I, and K_m is ~9.4 rather than ~9.0 at the higher temperature. An independent spectral assessment of the pK_a of the oxidized protein at 4 °C also gave a value of ~9.4 (data not shown). Thus at both temperatures the pK_a for reaction 3 was the same as the apparent pK_a of the ionization affecting K_m for O_2^- and K_d and K_I for azide.

Previously published results,[10] confirmed here, suggested that N_3^- and OH^- compete for the same coordination site on the Fe^{3+}. If this is true, then the K_I for competitive inhibition by OH^- should, like the K_I for N_3^-, be ~3-fold larger than its static binding constant (see Figure 4). This would have the effect of shifting the apparent pK_a in K_m vs. pH data to about $^1/_2$ pH unit above the directly measured pK_a of the oxidized enzyme. A difference of $^1/_2$ pH unit in these values would be easily discernable but is not observed (cf. lower dashed line in Figure 4). It would seem therefore that more than one pK_a may be affecting the kinetic parameters. We decided to test for the presence of an ionizing group linked to reduction of Fe^{3+}.

Proton Uptake on Reduction. Because reduced enzyme is colorless and EPR silent, we turned to redox potential measurements. It was recently reported[13] that the $E_m{}^7$ of FeSD was ca. +260 mV and that this varied with a slope of −60 mV in the pH range 6–10. The redox buffer used in this study was dichlorophenolindophenol (DCPIP) which has an $E_m{}^7 = +217$ mV.[32] Upon examining this system more closely, we found that DCPIP as well as other common electron transfer mediators react very slowly if at all with FeSD. Thus anaerobic, oxidized DCPIP did not react over several hours with reduced FeSD, nor did β-anthraquinone sulfonate, Fe^{+3}-EDTA, or ferricyanide. Similarly, reduced DCPIP would not reduce the oxidized enzyme. The enzyme could be reduced slowly by benzyl viologen radical (rate constant ~20 M^{-1} s^{-1}) and rapidly by dithionite. The enzyme could be reoxidized slowly by molecular oxygen and rapidly by superoxide. Full activity was retained throughout all of these procedures. Since measurement of a protein's redox potential requires that the redox buffers are equilibrating with both the electrode(s) and with the protein, the previously reported value must be incorrect. Until a suitable mediator is found, the redox potential of FeSD must be considered unknown.

However, it was possible to measure the uptake of protons on direct reduction in anaerobic, unbuffered solutions. When benzyl viologen radical was used as reductant, any pH change on reduction must be due to the protein. Titration back to the starting pH with standardized acid yielded the number of protons bound per iron, $\Delta H^+/Fe$. Dithionite, which releases two protons per electron given up,[33] could also be used. Standardized base was used to return the pH to its initial value, and $\Delta H^+/Fe$ was obtained as (2 - $\Delta OH^-/Fe$). Below pH 8, correction must be made for incomplete ionization of the sulfite produced by dithionite.[33] Titration of a mixture of ferricyanide and ovalbumin was used to check that this correction could be done properly. A typical experiment with the dismutase is shown in Figure 5. At each of the arrows shown in the upper panel, an amount of dithionite equivalent to 0.2 e/Fe was added. The pH and absorbance at

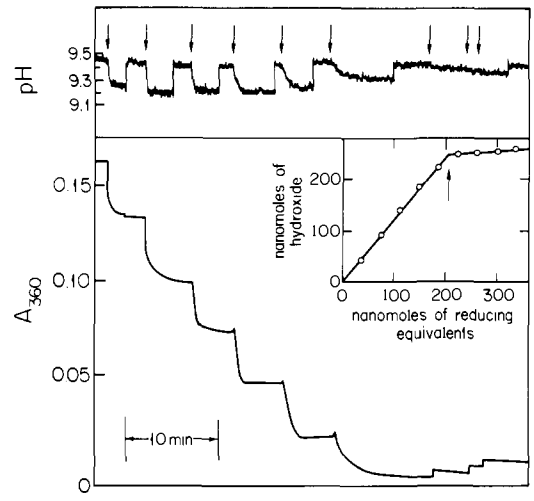

Figure 5. Demonstration of the linkage between reduction of oxidized iron superoxide dismutase and proton binding. Arrows in the upper panel indicate 5.1-μL additions of 10 mM dithionite to 1.5 mL of 130 μM FeSD in 0.05 M KCl initially at pH 9.5, 25 °C. Response of the absorbance at 360 nm and the pH are shown as a function of time. Several minutes after each addition of dithionite, 10 mM OH^- was used to return the pH to 9.5. In the inset, the total hydroxide added is plotted vs. the total reducing equivalents added; the arrow indicates the total protein bound iron present.

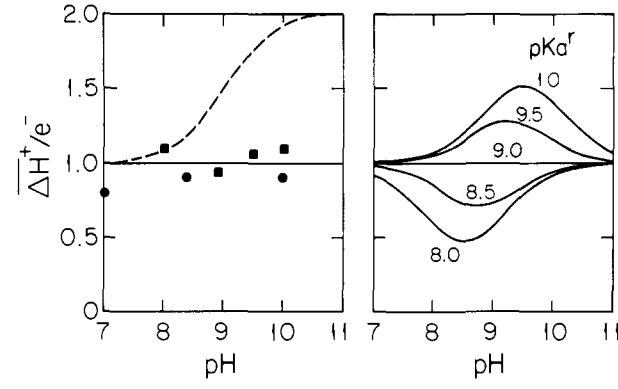

Figure 6. pH dependence of proton uptake on reduction of iron superoxide dismutase. The left panel shows data taken with dithionite as reductant (squares) and with benzyl viologen (circles). See text for calculation of $\Delta H^+/e^-$. The dashed line shows the behavior expected if the known pK_a of the oxidized enzyme is added to a constant uptake of one proton on reduction. The right panel shows the effect expected ($1 + (1 + [H^+]/K_a^o)^{-1} - (1 + [H^+]/K_a^r)^{-1}$) for compensating ionizations in oxidized and reduced enzyme: pK_a^o = 9.0 and pK_a^r as indicated.

360 nm (lower panel) were followed until reaction ceased, whereupon the standardized base was used to return the pH to its initial value. The inset of Figure 5 plots the uptake of protons on reduction vs. electrons added per iron. The expected stoichiometry of one electron per Fe^{3+} is found, and the results show clearly that one proton disappears from the medium on reduction of each Fe^{3+}.

This experiment was performed as a function of pH as shown in Figure 6 (left panel), and the data indicate that $\Delta H^+/Fe \simeq 1$ over the pH range 7 to 10. Considering that reaction 3 occurs with pK_a ~ 9, the data at low pH require that the pK_a of some group on the enzyme is linked to reduction of the iron. This could be a ferric ligand which is dissociated and protonated on reduction or it could be some ionizable group in close proximity to the iron. This group will be designated $-XH^+$ in its protonated state, keeping in mind that its net charge is unknown.

While previous results suggest that a water molecule bound to Fe^{3+} ionizes with pK_a ~ 9 to a bound hydroxyl ion, reaction 3, similar behavior is *not* expected for the Fe^{2+} ion. Thus, in the case of Fe^{3+}-EDTA, the bound water has pK_a ~ 7.6 while Fe^{2+}-EDTA has no comparable ionization below pH ~11.[3]

(30) The thermodynamics of self-dismutation reported here differ from the report of Bielski and Schwarz,[31] in which E_a = 2000 cal/mol. This is likely due to the differing pH at which the reaction was measured, pH 5 vs. pH 8.4 for this work. The previous data were taken close to the pK_a of superoxide (4.88) so that an appreciable fraction of the superoxide was present as HO_2. Since the reaction rate is proportional to the product $[HO_2][O_2^-]$, small changes in the pK_a with temperature produce little change in the product. Hence the temperature dependence of the intrinsic second-order rate of dismutation is obtained. In our measurements at high pH, the $[O_2^-]$ is essentially constant while $[HO_2]$ is changed by shifts in the pK_a, so we obtain a combined temperature dependence of the pK_a of superoxide and the intrinsic dismutation rate. The earlier results actually have some admixture of this effect since the measurement was not done at pK_a.

(31) Bielski, B. H. J.; Schwarz, H. A. *J. Phys. Chem.* **1968**, *72*, 3836–3841.

(32) Clark, W. M. "Oxidation-Reduction Potentials of Organic Systems"; R. E. Krieger Publishing Co.: Huntington, New York, 1972; p 405.

(33) Mayhew, S. G. *Eur. J. Biochem.* **1978**, *85*, 535–547 and references therein.

Scheme II

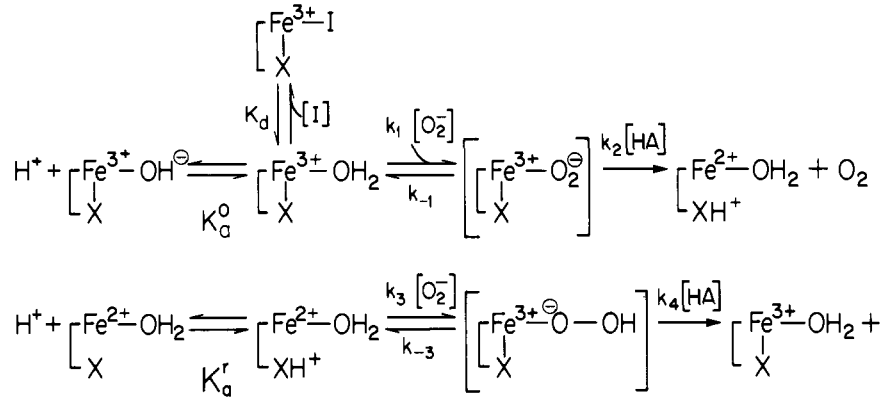

(18)

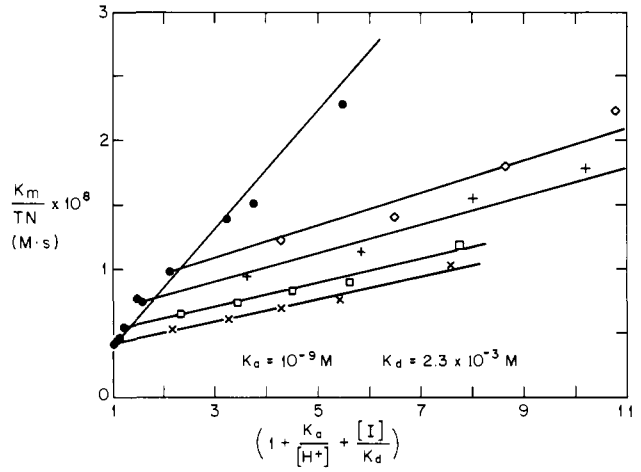

Figure 7. Effect of pH and azide on K_m/TN. Axes are described in the text and Table I. Filled circles show data taken at the following pH values (starting lower left): 7.49, 7.80, 8.08, 8.38, 8.69, 8.77, 9.05, 9.35, 9.44, 9.65. Open symbols show the effect of added azide at pH 7.49 (×), 8.38 (□), 8.69 (+), and 9.05 (◇). Conditions: 0.05 M buffer, 0.05 M KCl, 0.6 μM FeSD, 1 mM initial O_2^-, 25 °C.

Moreover, we did not find an example where chelated Fe^{2+} supports ionization of bound H_2O.[34] Therefore, we assume that upon reduction, Fe^{3+}-OH^- will bind a proton to form Fe^{2+}-OH_2. At high pH, protonation of both X and OH^- on reduction would give $\Delta H^+/Fe$ approaching 2 (dashed line of left panel, Figure 6), yet this is not observed. We deduce that there must be a compensating ionization in the reduced protein. The right panel of Figure 6 explores how close pK_a^r (the ionization in the reduced enzyme) must be to pK_a^o (the hydrolysis of oxidized enzyme) in order to match the observed data. These theoretical curves suggest that the two pK_a's must be nearly identical, and a conservative estimate would be that they are no further than 0.3 pH unit apart.

Catalytic Importance of Ionization in the Reduced Protein. The existence of this ionizable group in reduced protein raises the possibility that it may be important in catalysis. One plausible scheme which includes all known enzyme forms is shown in Scheme II (reaction 18). (The nature of the Michaelis complexes shown in brackets is speculative, and based on the above discussion, anion binding to Fe^{2+} was not included.) In this scheme, the reductive half of the reaction is presented as O_2^- binding to Fe^{3+}-OH_2 followed by combined electron transfer, proton uptake, and release of O_2. Anions and hydrolysis lower the concentration of Fe^{3+}-OH_2 by simple equilibrium processes, thereby preventing O_2^- from binding to the metal. In the oxidative half of the reaction, the binding of O_2^- to the Fe^{2+}-OH_2 form is combined with electron transfer and internal proton transfer to form the peroxo complex since these latter steps are likely to be quite rapid. The reverse reaction (k_{-3}) is expected to be very slow relative to k_3 due to the large free energy change on formation of peroxide from superoxide (cf. ref 2g). The breakdown of the peroxo complex is envisioned to require an additional proton to release neutral peroxide. Thus, on reduction the group X becomes protonated and XH^+ facilitates the binding of O_2^- to the reduced protein. Upon reoxidation the proton on XH^+ may be used to form the peroxide monoanion, although this is conjectural since this step never becomes rate limiting. Free protons cannot be involved in any process since this would require a reaction rate in excess of diffusion. Thus, at pH 10 and 25 °C, the TN has a value of 26 000 s^{-1}, implying a bimolecular association with H_3O^+ of 2.5×10^{14} M^{-1} s^{-1}. This is $\sim 10^3$ greater than the fastest reactions of H_3O^+ in water.[35] We have therefore proposed that a general acid (HA), most likely H_2O, is donating the necessary protons and that k_2 and k_4 are independent of pH. This scheme further assumes that O_2^- cannot bind to oxidized enzyme if another anion is directly bound.

The steady-state kinetics of reaction 18 are given by

$$-\frac{[dO_2^-]}{dt} = \frac{2[enz](1/k_2 + 1/k_4)^{-1}[O_2^-]}{\dfrac{(1/k_2 + 1/k_4)^{-1}}{\left[\dfrac{(1 + K_a^o/[H^+] + [I]/K_d)}{k_r} + \dfrac{(1 + K_a^r/[H^+])}{k_o}\right]^{-1}} + [O_2^-]} \quad (19)$$

and the ratio K_m/TN is particularly useful.

The expression describing the dependence of the kinetic parameter K_m/TN on $[H^+]$ and [I] is given by eq 20. The following

$$\frac{K_m}{TN} = \frac{1}{k_r}(1 + K_a^o/[H^+] + [I]/K_d) + \frac{1}{k_o}(1 + K_a^r/[H^+]) \quad (20)$$

illustrates how the dependence of K_m/TN measured at different $[H^+]$ and [I] concentrations can lend support to the catalytic importance of an ionizing group in the reduced protein.

Case I: K_a^r does not exist (or is uninvolved in catalysis), so the rightmost term of eq 20 reduces to $1/k_o$. The resulting expression predicts that in a plot of K_m/TN vs. $(1 + (K_a^o/[H^+]) + ([I]/K_d))$ data for any values of $[H^+]$ and [I] will fall on a single line. As shown in Figure 7, this is not true. When pH is varied in the absence of azide the data conform to a particular straight line while at constant pH and varying azide concentrations the data conform to straight lines having quite different parameters. This behavior is qualitatively consistent with the presence of pK_a^r.

Case II: Here we follow the suggestion from above (Figure 6) and allow $K_a^r = K_a^o$. The following analysis lends quantitative support for the catalytic importance of pK_a^r.

(34) Smith, R. M.; Martell, A. E. "Critical Stability Constants"; Plenum Press: New York, 1976; Vol. 4, pp 5 and 7.

(35) Eigen, M. *Angew. Chem. Int. Ed. Engl.* **1964**, *3*, 1–19.

Table II. Results of Plotting K_m/TN vs. $(1 + K_a^o/[H^+] + [I]/K_d)$

	case I ($K_a^r = 0$)	case II ($K_a^r = K_a^o$)	in general ($K_a^r \neq K_a^o$)	obsd[a]
intercept (no azide, low pH)	$1/k_r + 1/k_o$	$1/k_r + 1/k_o$	$1/k_r + 1/k_o$	4.0×10^{-9} Ms
slope (pH varied, no azide)	$1/k_r$	$1/k_r + 1/k_o$	$1/k_r + (K_a^r/K_a^o)/k_o$	4.4×10^{-9} Ms
slope (azide varied, fixed pH)	$1/k_r$	$1/k_r$	$1/k_r$	1.3×10^{-9} Ms

[a] Determined from the data in Figure 7.

In the absence of azide, a plot of K_m/TN vs. $(1 + (K_a^o/[H^+])$ should be linear with slope

$$\left[\frac{\partial(K_m/TN)}{\partial\left(1 + \frac{K_a^o}{[H^+]}\right)}\right]_{[I]=0} = \frac{1}{k_r} + \frac{1}{k_o}\left[\frac{\partial\left(1 + \frac{K_a^r}{[H_+]}\right)}{\partial\left(1 + \frac{K_a^o}{[H^+]}\right)}\right]_{[I]=0} \quad (21)$$

which is equal to $(1/k_r) + (1/k_o)(K_a^r/K_a^o)$ and reduces to $(1/k_r) + (1/k_o)$ when $K_a^o = K_a^r$. The data describing this line are shown as solid symbols in Figure 7, and the slope of the line is given in Table II.

In the presence of azide at constant pH, the data clearly fit different straight lines whem K_m/TN is plotted vs. $(1 + (K_a^o/[H^+]) + ([I]/K_d))$ as shown by the open symbols in Figure 7. The slope of these lines should be given by

$$\left[\frac{\partial(K_m/TN)}{\partial\left(1 + \frac{K_a^o}{[H^+]} + \frac{[I]}{K_d}\right)}\right]_{[H^+]} = \frac{1}{k_r} + \frac{1}{k_o}\left[\frac{\partial\left(1 + \frac{K_a^r}{[H^+]}\right)}{\partial\left(1 + \frac{K_a^o}{[H^+]} + \frac{[I]}{K_d}\right)}\right]_{[H^+]} \quad (22)$$

and because the differential term on the right is zero, the slope is equal to $1/k_r$.

Thus, from Table II

$$\frac{(1/k_r) + (1/k_o)}{1/k_r} = \frac{4.0 \times 10^{-9}}{1.3 \times 10^{-9}} = 3.1$$

and $k_r = 2.1k_o$. This is in remarkably good agreement with the prediction (Figures 2 and 3) that $k_r \simeq 2.0k_o$ (cf. ref 36).

We are now able to calculate the dependence of K_m, K_d, and K_I on pH as shown by the lines in Figure 4. For these conditions, the following parameters hold: TN = 8200 s^{-1}, $k_r = 4.7 \times 10^8$ M^{-1} s^{-1}, $k_o = 1.9 \times 10^8$ M^{-1} s^{-1}, $K_d = 0.83$ mM, and $K_a^o = 4.0 \times 10^{-10}$ M. The solid lines were calculated with an appropriate pH dependence of K_d, k_r, and k_o and by assuming $K_a^r = K_a^o$. The dashed lines were calculated similarly by assuming $K_a^r = 0$. The close correspondence of the solid lines to the experimental data

(36) One can also obtain numerical estimates of k_o, k_r, and K_a^r by plotting the data in a different manner. Equation 20 can be rewritten to

$$\frac{K_m}{TN} = \frac{1}{k_r}\left(1 + \frac{K_a^o[OH^-]}{K_w} + \frac{[I]}{K_d}\right) + \frac{1}{k_o}\left(1 + \frac{K_a^r[OH^-]}{K_w}\right)$$

A plot of K_m/TN vs. $[OH^-]$ in the absence of azide has slope $m_1 = 1/K_w$; $(K_a^o/k_r + K_a^r/k_o) = 4.3 \times 10^{-4}$ s and intercept $b_1 = 1/k_r + 1/k_o = 4.0 \times 10^{-9}$ Ms. At constant pH, a plot of K_m/TN vs. $[N_3^-]$ has slope $m_2 = 1/k_rK_d = 4.2 \times 10^{-7}$ s. Using $K_d = 2.3 \times 10^{-3}$ M and values of m_2 and b_1 leads to $k_r \sim 1 \times 10^9$ M^{-1} s^{-1} and $k_o \sim 3 \times 10^8$ M^{-1} s^{-1}. Using $K_a^o \sim 1 \times 10^{-9}$ M and the $K_w = 1 \times 10^{-14}$, values of m_1, k_r, and k_o yield $K_a^r \sim 1 \times 10^{-9}$ M.

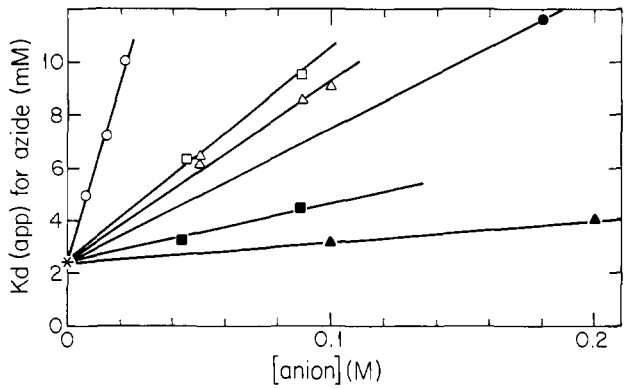

Figure 8. Anion inhibition of azide binding to iron superoxide dismutase. Symbols: *, 0.1 M TAPS, pH 8.4 only; ○, fluoride; □, thiocyanate; △, perchlorate; ●, cyanate; ■, chloride; ▲, sulfate. (A second point for 0.36 M cyanate conforms to the line.) Protein concentration was 130 μM as Fe, 25 °C.

Table III. Anion Binding and Inhibition

	N_3^-	F^-	SCN^-	ClO_4^-	CNO^-	Cl^-	SO_4^-
K_d (mM)	2.2	6.9	32	36	47	71	190
K_I (mM)	6.6	19	42	50		130	~300
K_I/K_d	3.0	2.8	1.3	1.4		1.8	1.6

provides additional support for the involvement of a ionizing group in the reduced protein.

Other Anions. The data shown in Figure 2 established that several anions act as competitive inhibitors of FeSD. Of these anions, only N_3^- and F^- bind directly to the ferric ion as evidenced by modification of its optical and EPR spectra (ref 9, results not shown), so that binding constants for the other anions cannot be measured directly. However, all these anions alter the binding constant for azide. For competitive binding, a linear relationship between the apparent binding constant for azide and the anion concentration should exist (expression 23)

$$K_d(app) = K_d + [anion]K_d/K_{anion} \quad (23)$$

where K_d corresponds here to the dissociation constant of N_3^- and K_{anion} to the dissociation constant of the competing anion, e.g., ClO_4^-. Data are shown for a number of anions in Figure 8. The binding constant for fluoride was determined both directly by titration and indirectly via its effect on the azide dissociation constant with very similar results (6.9 vs. 7 mM for K_d, respectively). The collected binding constants are presented in Table III.

Thus, these other anions compete with azide for a site on oxidized enzyme *which apparently cannot be the iron itself*, and this site is linked to azide binding to the iron. Temperature-jump studies of the azide-binding reaction[10] have demonstrated that a prior complex exists on the pathway to azide coordination of ferric ion (reaction 24)

$$N_3^- + \underset{X}{Fe^{3+}}\text{-}H_2O \overset{K_p}{\rightleftharpoons} [N_3^-\cdot\underset{X}{Fe^{3+}}\text{-}H_2O] \underset{k_{-5}}{\overset{k_5}{\rightleftharpoons}} \underset{X}{Fe^{3+}}\text{-}N_3^- \quad (24)$$

where $K_p = 20$ mM, $k_5 = 40\,000$ s^{-1}, and $k_{-5} = 8000$ s^{-1} at 8 °C and pH 7.4.[10] The simplest interpretation is that all anions can form a species similar to that shown in brackets, which results in competitive binding with azide.

Table III also presents inhibition constants measured directly for the anions studied. Both N_3^- and F^-, which are ferric ligands,

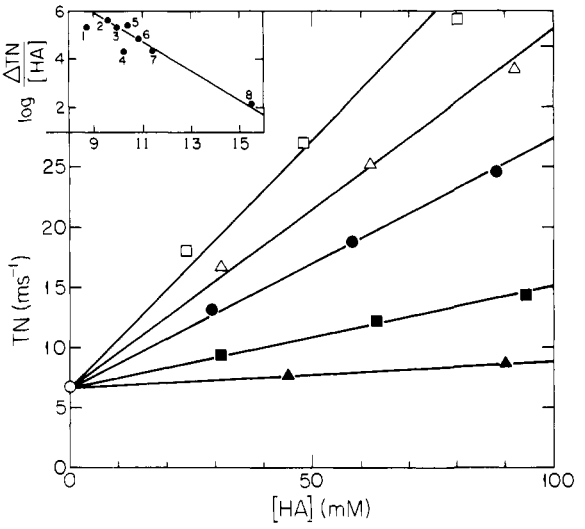

Figure 9. Effect of primary amines on TN. Concentrations after mixing: 0.1 M TAPS, pH 8.9 (at 4 °C), 0.1 M sodium sulfate, 10^{-4} M DETAPAC, 1 μM enzyme, 4 °C. Symbols show amine added: ○, no addition; □, taurine; △, glycine; ●, ammonium; ■, β-alanine; ▲, ethanolamine. Inset shows the logarithm of the slope of the lines in the main figure and of other amines vs. pK_a of the amine. Inset points: 1, glycylglyceine, 2, taurine; 3, glycine; 4, ethanolamine; 5 ammonia; 6, β-alanine; 7, methylamine; 8, water.

show the threefold difference between K_I and K_d which arises from differential binding to oxidized and reduced enzyme. However, for the other anions, K_I is closer to K_d, which implies that a similar site exists on the reduced enzyme. This site has been termed the anion binding pocket. If a particular anion binds to the pocket with equal affinity in both oxidized and reduced enzyme, then K_I should equal K_d. If there is strongly differential binding (oxidized being tighter), then a threefold difference between K_I and K_d should be observed (assuming $k_r = 2.0k_o$) as seen for N_3^- and F^-. The results for those anions which do not bind directly to the ferric ion in oxidized enzyme show K_I between 1.5 and 2 times K_d, implying binding to both oxidized and reduced enzyme with somewhat differing affinities.

The anions OCN^- and SCN^- are closely similar to azide, and together they predict that the dissociation constant for azide to the anion binding pocket alone should be between 30 and 60 mM at 25 °C. The T-jump result ($K_p \sim 20$ mM) was obtained at 8 °C and in the presence of 0.15 M chloride and so is not directly comparable, but it is certainly similar. Thus, the internal equilibrium constant between azide in the pocket and coordinated azide is at least 15. Although the previous conclusion that k_r is twice k_o was based on the assumption that azide binds solely to oxidized enzyme (Schemes I and II), the complete equation with differential binding (eq 19) reduces to eq 15 if there is more than a tenfold difference in binding between oxidized and reduced enzyme. Thus our result that k_r is twice k_o in FeSD appears to be valid.

The Rate-Limiting Step in Turnover. The maximum turnover number of FeSD was shown in Figure 2 to be independent of anions and pH. However, certain general acids can considerably increase the TN, and data taken at 4 °C for several primary amines are shown in Figure 9. These general acids did not change the rate of O_2^- binding to the enzyme (TN/K_m was essentially constant, data not shown). Other general acids such as carbonate and pyrophosphate also acted to increase TN, although their additional effect as anionic inhibitors made quantitative interpretation difficult.

The slopes of the lines in Figure 9 (in units of M^{-1} s^{-1}) represent the effective rates of proton donation by each general acid. The inset of Figure 9 shows a Brønsted plot of these slopes, including a point for water acting as a general acid (a TN of 6600 s^{-1} at 52 M H_2O gives 127 M^{-1} s^{-1}). The line in the inset of Figure 9 shows a Brønsted α of 0.6 which provides a reasonable fit to the data. Sterically hindered amines such as Good's buffers do not alter the TN, suggesting that the proton donor must approach the active site closely. The major conclusion made from these data is that water is probably acting as a general acid in the rate-limiting step (see Scheme II). If this is true then lowering the concentration of water in the medium should decrease TN.

Effect of Miscible Organic Solvents. We have briefly examined the effects of water miscible organic solvents on the steady-state kinetic parameters of FeSD. The protein is remarkably stable to denaturation by organic solvents. Thus, it retained full activity after overnight storage on ice in 70% methanol, 50% DMF, or 50% ethylene glycol in 0.1 M TAPS, pH 8.9. These organic solvents are very poor proton donors, so their inclusion should lower the activity of water and hence lower the TN. Data for TN in 0.1 M TAPS, pH 8.9, at 6 °C were 6600, 5700, 4900, 4300, and 3200 s^{-1} in 0, 10, 20, 30, and 40% methanol, respectively, while K_m remained constant. Similar decreases in TN occurred with ethylene glycol. Analysis of the velocity traces gave no evidence for denaturation during catalysis. The decline in TN is greater than simple dilution of water could predict, especially at low organic solvent concentrations. While the addition of organic cosolvents certainly has much more effect than merely diluting water,[37,38] these data are consistent with proton donation by water in the limiting step of catalysis.

Discussion

Scheme I and its attendant steady-state velocity expression describes superoxide dismutase activity in terms of three processes: binding of superoxide on the metal, a redistribution of electronic charge involving movement of protons and electrons, and the release of products. This scheme should be applicable to all superoxide dismutases. In the case of the Cu/Zn-protein the rate-limiting step is apparently binding and no saturation is observed even at very high $[O_2^-]$. The velocity of the reaction therefore is always given by the equation

$$-d[O_2^-]/dt = (1/k_1 + 1/k_3)^{-1}2[Cu][O_2^-] \qquad (25)$$

where $(1/k_1 + 1/k_3)^{-1}$ is the effective second-order constant of O_2^- binding to the protein. In the case of Fe- and Mn-proteins, general expression 9 accounts for the observed saturation effects and yields kinetic constants characteristic of binding reactions and of charge rearrangement or product release. To the extent that the individual proteins undergo catalytically relevant ionizations or inhibition by anions, the expression can be modified to account for these effects as illustrated by eq 19.

The following information has been used to suggest a mechanism of the iron superoxide dismutase: a cyclic redox process,[2c] the occurrence of simple saturation kinetics, the hydrolysis of Fe^{3+}-OH_2 with pK_a° ~9,[10] competitive inhibition by anions such as N_3^- and F^- which bind directly to Fe^{3+}, a strong linkage between reduction of Fe^{3+} and binding a proton, and rate-limiting proton donation from general acids in the medium. The mechanism proposed in Scheme II accounts for present observations and conforms with the known chemistry of O_2^- and of $Fe^{3+/2+}$ coordination complexes. The velocity expression 19 which incorporates hydrolysis of Fe^{3+}-OH_2, binding of anions to Fe^{3+}, and ionization of the unidentified group X in the reduced protein predicts simple saturation behavior and accounts for the pH dependence of K_m and TN and for competitive inhibition by anions.

The steady-state kinetic analysis using expression 19 yielded information on both O_2^- binding and subsequent processes. The binding of O_2^- to the oxidized protein appears to occur only to the Fe^{3+}-OH_2 form. Thus, anions such as OH^-, N_3^-, and F^- which also bind to Fe^{3+} act as competitive inhibitors; they have no effect on the charge redistribution and proton transfer reactions. The presence of an ionizable group X in reduced protein was deduced from two effects: the strong linkage between e^- and H^+ binding

(37) Douzou, P. "Cryobiochemistry"; Academic Press: London, 1977.
(38) Addition of organic solvents increases the superoxide self-dismutation rate. The effect is small below 20% MeOH, but it increases greatly above 30% MeOH (6× faster at 40%). We interpret this as an upward shift in the pK_a of superoxide as the dielectric constant of the medium is decreased, leading to an increased rate of dismutation. The size of the effect correlates well with the dielectric measurements of Douzou.[37]

to the protein and from the kinetic data which suggested OH^- was "binding" to both oxidized and reduced forms of the enzyme. The binding rate of O_2^- to the reduced form of the protein appears to be determined by the presence of XH^+. Since we suspect electron transfer from Fe^{2+} to coordinated O_2^- to be very rapid, we have combined two processes in step 3 of Scheme II: O_2^- binding to Fe^{2+} and charge rearrangement to form the Fe^{3+} peroxo complex. The fact that TN is independent of pH suggests that charge rearrangement in this process never becomes rate limiting. Since it is reasonable that k_{-3} is much smaller than k_4 then $k_0 \simeq k_3$. This argument suggests that release of peroxide from the Fe^{3+}, step 4, may be the slow step in reoxidation by O_2^-.

The finding that general acids such as primary amines substantially increase the value of TN is good evidence that proton transfer is the rate-limiting step in catalysis. Clearly hydronium ions are not involved, and we suggest H_2O is the usual proton donor in steps 2 and 4 of Scheme II. Indeed, a Brønsted value of $\alpha = 0.6$ nicely connects the water point in the inset of Figure 9 with the cluster of points relating to the primary amines. The similarity of α in this system to that previously observed for the general acid catalyzed decay of EDTA-Fe^{3+}-$^-$O-OH complex[3] suggests that the rate-limiting step in the overall reaction may be the general acid assisted decay of a Fe^{3+} peroxo intermediate (cf. ref 39). Further but less convincing evidence that H_2O is directly involved is suggested by the substantial decrease in TN which occurs when the concentration of H_2O is lowered with organic solvents. However, kinetically important changes in redox potentials resulting from changes in solvent composition cannot be ruled out.

Inhibition by anions proved to be quite complex. An earlier study[10] showed that azide binding to the Fe^{3+} occurred in two steps. The first step was thought to be at a site near but not on the Fe^{3+} because the anion caused no spectral change upon binding. The second step involved direct association of the anion with Fe^{3+} as it changed its optical spectrum. These results led to the suggestion that anions become bound first in a "pocket" near the Fe^{3+} and then moved to the metal. The present results are also consistent with a pocket near the iron to which O_2^- binds before reaching the active site. Thus, anions such as ClO_4^- and SCN^- which cause no perturbation of Fe^{3+} spectral properties are thought to inhibit by occupying this pocket. A similar suggestion was also made by Benovic et al.,[43] and their results are consistent with ours. We have chosen to interpret our data under the assumption that anions do not bind to Fe^{2+}, and this is appropriate for N_3^- and F^-. However, the weaker inhibition by the other anions is more complicated, and the data of Table III suggest that the affinity of the pocket for anions may be different in the oxidized and reduced forms of the protein. Such behavior would be consistent with the group XH^+ affecting the properties of the pocket.

Acknowledgment. We thank Ms. Carol J. Nettleton for purification of proteins.

Registry No. SD, 9054-89-1; Fe, 7439-89-6; N_3^-, 14343-69-2; F^-, 16984-48-8; SCN^-, 302-04-5; ClO_4^-, 14797-73-0; CNO^-, 661-20-1; Cl^-, 16887-00-6; SO_4^-, 14808-79-8; $HCOO^-$, 71-47-6; superoxide, 11062-77-4.

(39) The mechanism for FeSD proposed in Scheme II bears some similarities to widely discussed mechanisms for Cu/ZnSD. Thus, the protonation of X might be considered analogous to the protonation of the bridging imidazolate group of the Cu-protein. However, XH^+ of FeSD is apparently involved in O_2^- binding whereas the protonated, Zn-bound imidazole was thought to assist in proton transfer.[40] Recently, O'Neill et al.[41] have shown that the Zn-free protein has the same specific activity as the holoprotein. However, because the velocity of the catalyzed reaction measures only the rates at which O_2^- binds to the protein, this result does not exclude the possibility that the bridging imidazolate transfers protons to the metal bound O_2^- (cf. ref 42).

(40) McAdam, M. E.; Fielden, E. M.; Lavelle, F.; Calabrese, L.; Cocco, D.; Rotilio, G. *Biochem. J.* **1977**, *167*, 271–274.

(41) O'Neill, P. O.; Fielden, E. M.; Cocco, D.; Calabrese, L.; Rotilio, G. In "Oxy-radicals and their Scavenger Systems. Volume I. Molecular Aspects"; Cohen, G., Greenwald, R. A., Eds.; Elsevier Press: New York, 1983; pp 316–319.

(42) Fee, J. A.; Ward, R. L. *Biochem. Biophys. Res. Commun.* **1976**, *71*, 427–437.

(43) Benovic, J.; Tillman, T.; Cudd, A.; Fridovich, I. *Arch. Biochem. Biophys.* **1983**, *221*, 329–332.